Research Article
Sciences of Pharmacy

Development of Chitosan-Based Antimicrobial Hydrogel Incorporating Polyvinylpyrrolidone and PHMG

Ivan Ivanov, Denis Shatalov

[The author informations are in the declarations section. This article is published by ETFLIN in Sciences of Pharmacy, Volume 3, Issue 4, 2024, Page 220-229. https://doi.org/10.58920/sciphar0304289]

Received: 03 October 2024
Revised: 12 December 2024
Accepted: 19 December 2024
Published: 27 December 2024

Editor: Adeleye Ademola Olutayo

Keywords: Wound healing, Bandage, Drug release, Polymers.

Abstract: This study focuses on the development of a chitosan-based hydrogel incorporating polyvinylpyrrolidone and polyhexamethylene guanidine hydrochloride for the rehabilitation of damaged and contaminated skin. The thermal properties of chitosan-containing films were characterized by measuring the glass transition temperature (T_g) using differential scanning calorimetry. Due to challenges in accurately determining the Tg of chitosan from experimental and literature data, an additional method, dynamic mechanical analysis, was employed. Using the literature value for the Tg of polyhexamethylene guanidine hydrochloride, the transitions of the components were determined. The estimated sorption capacity of the developed hydrogel showed that the inclusion of polyhexamethylene guanidine hydrochloride reduced the moisture content, as expected. However, the overall behavior of the hydrogels remained similar. Vapor permeability, an important factor in wound healing, was also evaluated. Antimicrobial testing revealed no activity for the chitosan control sample despite some reports in the literature, while the samples containing polyhexamethylene guanidine hydrochloride exhibited superior antimicrobial efficacy. These findings suggest that the incorporation of polyhexamethylene guanidine hydrochloride and polyvinylpyrrolidone significantly enhances both the mechanical strength and antimicrobial potential of chitosan-based hydrogels, positioning them as promising candidates for the treatment of contaminated wounds.

Introduction

The development of effective wound dressings remains a pressing issue in modern medicine. Traditional dressing materials can cover and protect the wound from infection and promote scab formation. However, they may adhere to the wound surface and cause secondary mechanical damage. Moreover, they lack antibacterial properties and do not create a moist environment conducive to wound healing. As a result, the wound becomes dehydrated, leading to the loss of biologically active substances, which prolongs the healing process (1-3).

Hydrogel dressings have garnered significant attention due to their unique properties that promote optimal wound healing. These dressings provide balanced moisture retention, exudate absorption, and infection protection, which is especially important in the treatment of burns, trophic ulcers, diabetic, and post-traumatic wounds. Most hydrogels are based on the inclusion of synthetic or natural polymers forming a three-dimensional network containing an aqueous medium. Among synthetic polymers, poly(meth)acrylates, polyethylene glycols, poly(vinyl alcohols), poly(vinylpyrrolidones) (PVP), polylactic-co-glycolic acid, and poly(urethanes) are of great importance. In contrast, natural polymers are mainly represented by polysaccharides, such as hyaluronic acid, alginate, or chitosan (CHS), and proteins, such as albumin, collagen, or elastin. Hydrogels, with their three-dimensional crosslinked network structures, possess physical and chemical properties similar to human tissues (4, 5).

CHS is a naturally derived polymer. Due to its biodegradability, non-toxicity, excellent film-forming ability, and antimicrobial and antifungal activity, CHS-based materials play an important role in various industries. Despite its numerous advantages, CHS films also have certain drawbacks, such as low vapor permeability and poor mechanical and thermal properties. The most effective method for producing more durable CHS coatings is polymer blending, particularly with PVP (6, 7).

PVP, in turn, is a synthetic polymer known for its biocompatibility, non-toxicity, and hydrophilic properties. It is widely used in controlled drug release, wound dressings, and tissue engineering. Additionally, PVP is a water-soluble polymer that positively impacts absorption, viscosity, solubilization, and condensation and can form mixtures with CHS. PVP can form hydrogen bonds with CHS through the interaction between the amino and hydroxyl groups of CHS and the carbonyl group of PVP. Aldana *et al*. reported the fabrication of CHS/genipin/PVP films for controlled drug release (8-12).

The use of polyhexamethylene guanidine hydrochloride (PHMG-H) in such film coatings could be highly effective, as this polymer is known for its broad-spectrum antibacterial activity and even regenerative properties. Furthermore, this agent exhibits fewer side effects on human skin (13, 14). In the literature, there is only one study mentioning the side effects of topical PHMG-H application, where sensitization occurred in a patient over 1–2 months of frequent use of a non-alcoholic disinfectant containing PHMG-H at a concentration of 0.1–1%. However, it is important to note that the patient had a history of irritant dermatitis (15). This study aims to develop and characterize a CHS-based hydrogel dressing by modifying its strength and antibacterial properties through the incorporation of PVP and PHMG-H.

Experimental Section

Materials

PVP (Weight Average Molecular Weight: 58 kDa, K-Value Viscosity: 29−32) was supplied by Ashland, USA. Food-grade water-soluble CHS (deacetylation degree (DD): 75−95%, average molecular weight: 1.0 – 30.0 kDa, mass fraction of moisture is ~5%.) was supplied by Bioprogress LLC, Russia. PHMG-H was supplied by Polisept LLC, Russia. Glycerol (no less than 99%) was supplied by TD Khimmed LLC, Russia. Glacial acetic acid (no less than 99.8%) was supplied by Component-Reactive LLC, Russia. Sodium hydroxide (no less than 98.0%) was supplied by CDH, India.

Preparation of hydrogels

Twenty grams of PVP were dissolved in 200 mL of distilled water with mechanical stirring at room temperature until the component was fully dissolved. The solution was then alkalized using a 10% sodium hydroxide solution to a pH of 9.0 ± 0.5, and 20 mL of glycerol was added while stirring. The resulting mixture was poured into glass containers, sealed with rubber stoppers, crimped with aluminum caps, and autoclaved in a steam sterilizer for 8 min at a pressure of 1 kgf/cm² and a temperature of +119.6 °C. In a separate container, 1.0−3.0 g of CHS (depending on the experimental sample) were dissolved in 100 mL of distilled water with mechanical stirring for 15−20 min at a speed of 430 rpm. Then, while reducing the stirring speed to 170 rpm, 2.1 g of glacial acetic acid and 0.8 g of PHMG-H were added to the suspension. After vigorous stirring, the solution was neutralized with alkali to a pH of 6.1, and stirring was resumed at a speed of 430 rpm for 5−10 min.

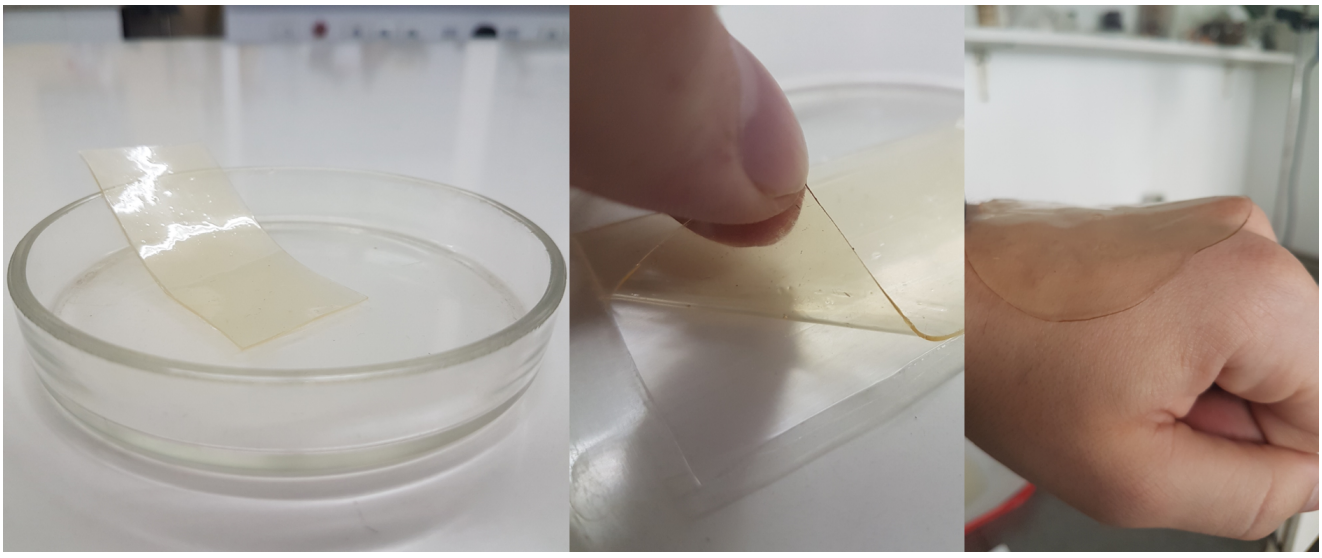

Figure 1. Hydrogels based on CHS/PVP/PHMG-H.

Table 1. Compositions of experimental hydrogel samples.

Sample	Ingredients, Gramm				
	PVP	Glycerol	CHS	PHMG-H	Acetic acid
Control	10.0	25.2	2.0	-	2.1
S1/0.8			1.0	0.8	
S2/0.8			2.0		
S3/0.8			3.0		

The resulting PVP and CHS/PHMG-H solutions were combined at room temperature and mixed intensively with mechanical stirring until a homogeneous solution was obtained for 10 min at a speed of 430 rpm. The final mixture was alkalized to a pH of 6.2−6.3. The resulting mass was applied to a molding vessel with wall heights of approximately 1.5 mm, with a dense polyethylene film substrate placed in advance and dried for 24 h. The hydrogel formulations are listed in **Table 1**, with the pure PVP/CHS hydrogel prepared as the control. The overall appearance of the hydrogels is shown in **Figure 1**.

Characterization of hydrogels

Differential Scanning Calorimetry (DSC)

To determine the glass transition temperature (T_g) of CHS, the analysis was performed using a universal differential scanning calorimeter NETZSCH DSC 204 F1 Phoenix®, Germany. The samples were scanned from 25℃ to 250℃ at a rate of 10℃/min under a nitrogen atmosphere.

Dynamic Mechanical Analysis (DMA)

The analysis was conducted using a dynamic mechanical analyzer NETZSCH DMA 242 C®, Germany. Film strips with polyethylene backing, measuring 10 x 6 mm and having a thickness of 0.32 mm (for the sample with 2% CHS concentration) and 0.37 mm (for the sample with 3% CHS concentration), were prepared as samples for DMA. The sample S1/0.8 could not be secured in the device's cuvette due to its low mechanical strength and, therefore, was not analyzed.

Swelling Behaviors

To assess the material's sorption capacity, the swelling of the samples was measured gravimetrically. Experimental samples, dried to constant weight, with a diameter of 21 mm and weighing between 0.20 and 0.27 g, were placed in custom-made aluminum dishes. The dishes were labeled and placed on a perforated porcelain platform inside a desiccator, where constant air humidity was maintained due to the presence of water in the lower part of the vessel. The experiment was considered complete when the weight of the dish with the material became constant. Two measurements were conducted for each of the four samples to average the results. Subsequently, the sorption isotherm was plotted, and the swelling degree of the material was calculated using the following formula:

$$\alpha = \frac{m - m_0}{m_0} \times 100\% \quad \textbf{Equation 1}$$

Where m is the mass of the swollen sample and m_0 is the initial mass of the sample in grams.

Water Vapor Transmission Rates

The method for determining water vapor permeability involves creating a difference in water vapor pressure on both sides of the tested sample and measuring the amount of water vapor passing through a unit area of the sample over a unit of time. To measure vapor permeability, templates with a diameter of 2.5 cm were cut from the obtained film material so that the edges of the sample matched the outer diameter of the gasket. The bottom of a corrosion-resistant beaker was filled with 25 ± 1 mL of distilled water. A rubber gasket was placed on the working opening and shoulder of the beaker, on top of which the medical device sample was laid. The beaker was tightly sealed with a lid to secure the tested sample (16). The beakers with samples were weighed on electronic analytical scales. The beakers containing the film materials were placed in a desiccator, which was then placed in a thermostat and kept at a temperature of 37 °C for 1 h Upon completion of the experiment, the masses of the beakers were recorded before and after the thermostat. The vapor permeability of the samples was then calculated using the following formula:

$$\mu = \frac{m_1 - m_2}{(\pi r^2) \times \tau} \quad \textbf{Equation 2}$$

Where m_1 is the mass of the weighing bottle before thermosetting, m_2 is the mass of the weighing bottle after thermosetting, π is a mathematical constant, the ratio of the circumference to its diameter (≈ 3.14), r is the radius of the sample, τ is the time of the experiment.

Antimicrobial testing

The determination of the antimicrobial activity of the samples was carried out using the disk diffusion method. For this, the strain of obligate methylotrophic bacteria *Methylophilus quaylei*, under the number MT B-2338T, was used (17). Although *Methylophilus quaylei* is an obligate methylotrophic bacterium not associated with human infections, it can form biofilms, making it resistant to antibiotics. For example, the *Methylophilus quaylei* MT strain was resistant to polymyxin B at a concentration of 0.01 µg/mL, even though polymyxin B is FDA-approved for serious infections caused by multidrug-resistant gram-negative bacteria. Therefore, this bacterium is suitable for modeling the antimicrobial activity of both CHS and PHMG-H (18, 19).

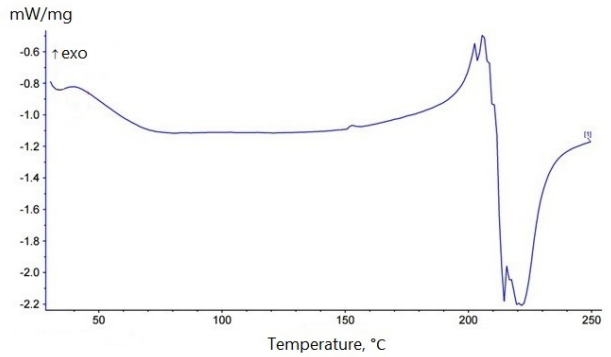

Figure 2. DSC thermogram of CHS used in the formation of hydrogels.

Table 2. Literature data about T_g of CHS.

Source	T_g, K	T_g, °C
Ogura et al. (1980) (24)	423.15	~150
Ahn et al. (2001) (25)	434.15	161
Pizzoli et al. (1991) (26)	493.15	220
Sakurai et al. (2000) (27)	476.15	203

The cultivation conditions used were a solid nutrient mineral medium containing 1% methanol and 1.5% Bactoagar (USA) (20). Twenty microliters of a 24-hour inoculum of *Methylophilus quaylei* were applied to a 95 mm diameter Petri dish containing 20 mL of solid nutrient medium and evenly spread across the surface. Immediately after this, two filter paper discs with a diameter of 5 mm were placed on the surface of the agar and pressed down with sterile tweezers. Then, 5 µL of the control solutions K1 (aqueous solution of 0.8% PHMG-H) and K2 (Control according to **Table 1**) were applied to the paper discs. Similarly, hydrogel samples numbered 0−3 were placed on the agar. Sample K2 was duplicated with hydrogel number 0 to confirm or refute the antibacterial activity of CHS. The Petri dish with the samples was placed in a thermostat and incubated at 28 °C for 24−48 h. The size of the inhibition zones was determined by measuring the distance in millimeters from the edge of the disc to the start of the bacterial lawn.

Results and Discussion

Thermal properties of CHS

The T_g of CHS typically ranges from 140 to 150 °C, although some studies suggest it may span from 100 to 200 °C. Research indicates that the T_g of CHS containing 8 to 30% water can decrease to as low as 30 °C (21-23). The T_g measurement of the CHS used in this study, obtained via DSC, is presented in **Figure 2**.

As shown, determining the T_g is challenging. The literature also indicates that pinpointing a specific temperature range for the glass transition is difficult due to significant variability in the data and a lack of consensus among researchers regarding the number of T_g values characteristic of amino polysaccharides. **Table 2** presents the T_g values reported by different researchers.

Several studies claim that CHS is characterized by two T_g ranges associated with the presence of microdomains in the macromolecule with varying degrees of order. The first glass transition range lies between 340−360 K (66.85−86.85 °C), while the second is between 400−420 K (126.85−146.85 °C) (28-30). In the DSC curves of one of the published studies, a single transition was detected, with the temperature ranges presented in **Table 3** (31).

Table 3. Literature data about T_g of CHS according to (31).

M, kDa (DD)	T, K	Transition temperature range, K	T, °C	Transition temperature range, °C
2 (97%)	363.9	327−369	90.75	53.85−95.85
7.7 (98.5%)	357.3	349−366	84.15	75.85−92.85
18.8 (90.4%)	356.9	330−374	83.75	56.85−100.85
180 (−)	338.1	316−356	64.95	42.85−82.85
200 (82%)	334.2	327−351	61.05	53.85−77.85
200 (83%)	338.2	318−354	65.05	44.85−80.85
500 (60%)	316.8	306−325	43.65	32.85−51.85
500 (80.5%)	320.5	304−346	47.35	30.85−72.85
500 (90%)	326.2	306−382	53.05	32.85−108.85
700 (80%)	312.6	301−331	39.45	27.85−57.85

Note: M – molecular weight. DD – deacetylation degree.

Based on the results presented in **Figure 2** and the following (32), it is undeniable that determining the exact T_g of CHS is quite challenging. According to data (33), the thermogram of CHS shows a broad endothermic peak between 70 and 80 °C, which is attributed to the evaporation of residual solvents absorbed from the atmosphere. This observation may reflect the conditions of the current study. It is suggested that at approximately 205 °C, the biopolymer undergoes significant degradation. Based on the entire data set presented (24-27), it can be inferred that the T_g likely falls within the range of 149.85–160.85 °C, as indicated in references (24, 25).

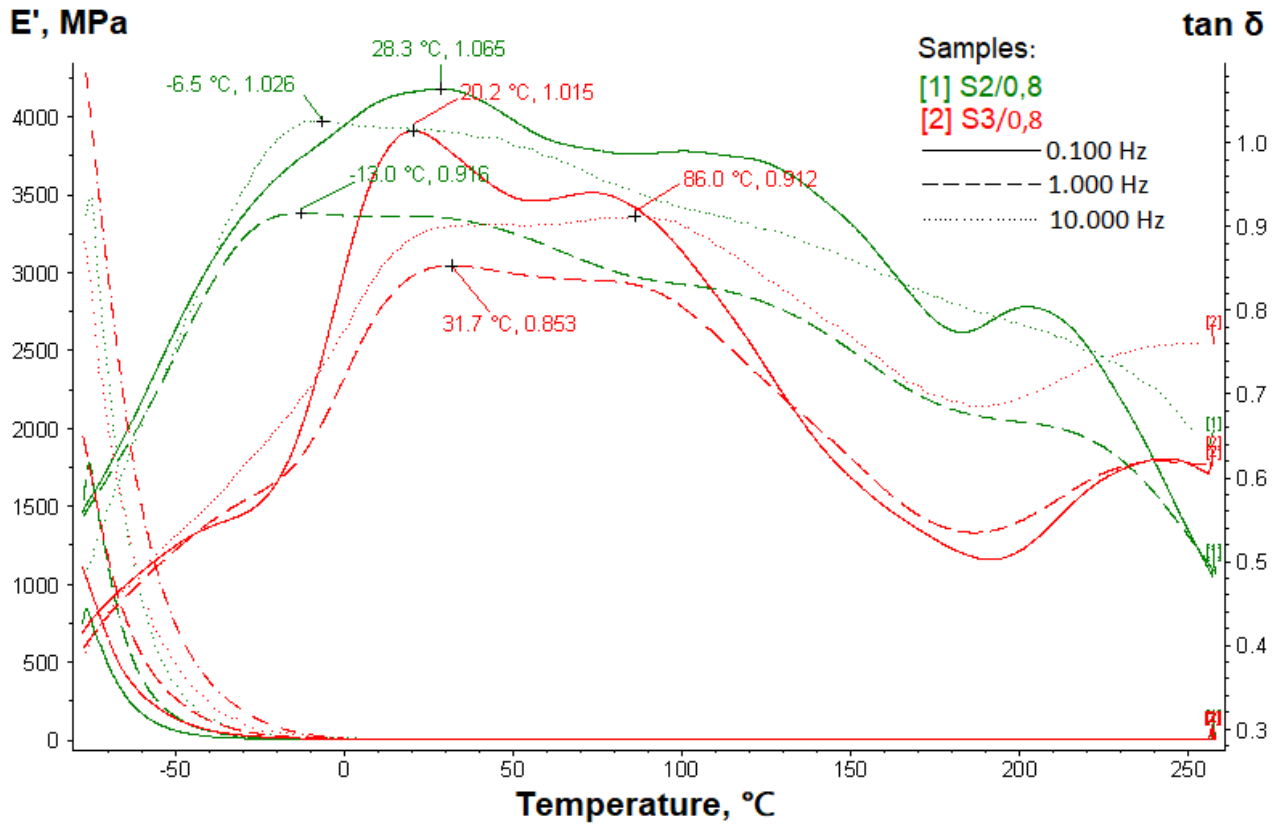

Figure 3. DMA thermogram of S2/0.8 and S3/0.8 samples.

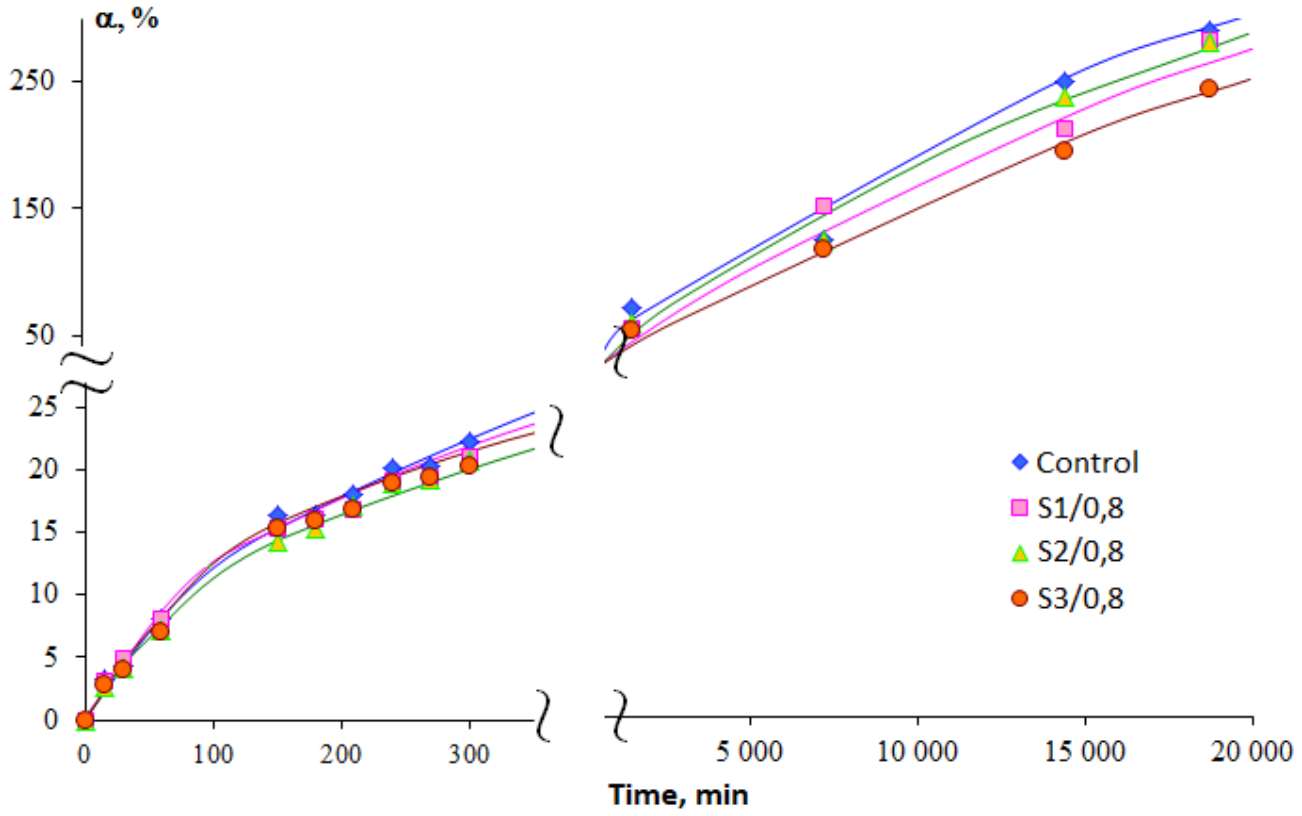

Figure 4. The swelling kinetics of hydrogel samples as a result of the sorption capacity study, where α represents the degree of swelling in %.

Dynamic mechanical properties

DMA is often used to confirm or supplement DSC results (34). DSC can be used on samples that have different structures (amorphous and crystalline). However, DSC may not be suitable for the analysis of network structures due to the complexity of the identification process (35). DMA is generally a more sensitive transition detection technology than DSC and Differential Thermal Analysis (DTA) (36).

Two samples (S2/0.8 and S3/0.8) were analyzed using DMA (**Figure 3**). The sample S1/0.8 turned out to be very brittle and prone to breaking, to the extent that it could not be secured in the instrument's cuvette.

It can be assumed that in the S2/0.8 and S3/0.8 samples, the glass transition of CHS and PHMG-H occurs within a similar temperature range, as it is reported that the T_g of PHMG-H is 65–85 °C (37, 38). The temperature peaks at ~86 °C for the S3/0.8 sample, possibly confirming the active involvement of PHMG-H in the glass transition. In contrast, the peaks at lower temperatures (0–30 °C) may be associated with the relaxation of the amorphous regions of the polymer matrix consisting of CHS and PHMG-H, as well as the possible influence of moisture (39). PVP likely exhibits glass transition at higher temperatures, which is consistent with literature data indicating that the T_g of this component can range from 100 °C to 175 °C depending on the molecular weight (40).

Kinetics of hydrogel swelling

Understanding the swelling dynamics and diffusion processes of hydrogels is critical to improving their performance in drug delivery, tissue engineering, and wound healing. The swelling process of CHS under conditions of formed chemical crosslinks or in their absence is explained by the theory of swelling of polymer networks, including crystalline structures and physical entanglements. (41). In the study (42), the swelling property of non-crosslinked CHS hydrogel increased with time, which was attributed to the hydrophilic nature of CHS, which is a result of the primary -OH group in CHS and the flexible matrix nature. The degree of crosslinked CHS was lower than that of non-crosslinked CHS hydrogel. **Figure 4** shows the sorption curve of CHS/PVP/PHMG-H hydrogels.

The data indicate that the Control has a higher capacity compared to the samples containing CHS along with PHMG-H. It is possible that PHMG-H, being a polycation, may interact with the amino groups of CHS, reducing its moisture sorption capacity, as ionic interactions can densify the structure and decrease the availability of hydrophilic groups in CHS. Overall, the hydrogels containing CHS and PHMG-H behave similarly, with PHMG-H, as expected, reducing the sorption capacity. In the short term (0–5 h), the hydrogel S1/0.8 absorbed more moisture than the hydrogels S2/0.8 and S3/0.8. However, in long-term testing (17 h and beyond), the best sorption capacity after Control was shown by the sample S2/0.8.

Water vapor transmission evaluation

Values of 2000–2500 g/m^2/day provide a guaranteed range for the release of sufficient exudate and prevention of wound dehydration (43). However, the water vapor transmission rate of a number of commercially available wound dressings, including hydrogels, had a wide range of 76–9360 g/m^2/day over 24 h (44). According to the Russian standard applicable to sterile and non-sterile medical devices that adhere to the skin due to an adhesive layer or the adhesive properties of the material itself, the water vapor permeability must be at least 1.5 mg/cm²/h (45). The results of the vapor permeability measurements are shown in **Table 4**.

Table 4. Vapor permeability values in samples of hydrogels.

Sample	Average vapor permeability, mg/cm^2/h
Control	7.93
S2/0,8	8.34
S3/0,8	6.39

It should be noted that sample S1/0.8 was not tested, as it exhibited poor mechanical properties, which was also confirmed in the dynamic mechanical properties section. The comparison of vapor permeability among the samples revealed that the most permeable sample is S2/0.8, while the least permeable is S3/0.8. The polymer network may be more tightly formed in samples containing CHS and PHMG-H. However, due to the formation of ionic interactions, vapor permeability may improve, as a denser network could facilitate more active vapor exchange, especially if water is not as effectively retained in the structure, as indicated by the results obtained in the kinetics of hydrogel swelling section.

Antimicrobial activities of hydrogels

Although the sample S1/0.8 was formally excluded from further testing, it was of interest to investigate its potential antimicrobial activity against *Methylophilus quaylei*. **Figure 5** shows the inhibition zones of the hydrogels against *Methylophilus quaylei*.

Based on the conducted study, the sizes of the clear zones, measured in millimeters, were determined, indicating the inhibition of pathogenic microorganisms by the samples. The results are presented in **Table 5**.

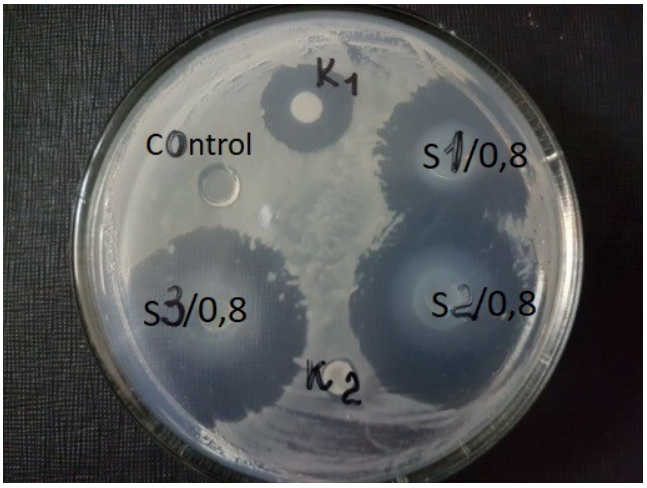

Figure 5. Photos of inhibition zone of hydrogels against *Methylophilus quaylei*.

Table 5. Inhibition zone size of hydrogel samples.

Sample	Inhibition zone size, mm
K1	5.5
K2	-
Control	-
S1/0,8	10.5
S2/0,8	15
S3/0,8	14.5

The samples S2/0.8 and S3/0.8 exhibited the most pronounced antimicrobial activity, as evidenced by the largest clear zones. In the conditions of the conducted experiment, the antimicrobial activity of CHS, which is mentioned in the literature, was not confirmed.

Conclusion

In conclusion, the CHS/PVP/PHMG-H hydrogel was developed using a solution mixing method with stepwise pH adjustment. Complementary DSC and DMA methods were used to study the thermal properties of the material, which helped to identify the phase transitions more clearly. Based on the presented data, the S2/0.8 sample demonstrated balanced mechanical, sorption, and vapor permeability properties. In addition, the S2/0.8 sample demonstrated the best antibacterial properties, as indicated by a large inhibition zone of pathogenic microorganisms. Thus, the developed hydrogel can be useful for biomedical applications. Having acceptable vapor permeability, it is assumed that this dressing will better promote wound healing processes, and the manifestation of antibacterial properties by the material will exclude the occurrence of septic processes.

Abbreviations

CHS = chitosan; PVP = polyvinylpyrrolidone; PHMG-H = polyhexamethylene guanidine hydrochloride; DD = deacetylation degree; DSC = differential scanning calorimetry; T_g = glass transition temperature; DMA = dynamic mechanical analysis; M = molecular weight.

Declarations

Author Informations

Ivan Ivanov
Affiliation: MIREA – Russian Technological University.
Contribution: Conceptualization, Data Curation, Investigation, Methodology, Writing - Original Draft.

Denis Shatalov
Affiliation: MIREA – Russian Technological University.
Contribution: Project administration, Writing - Review & Editing.

Conflict of Interest

The authors declare no conflicting interest.

Data Availability

The unpublished data is available upon request to the corresponding author.

Ethics Statement

Not applicable.

Funding Information

Not applicable.

References

1. Yang, C., Liu, G., Chen, J., Zeng, B., Shen, T., Qiu, D., Huang, C., Li, L., Chen, D., Chen, J., Mu, Z., Deng, H., & Cai, X. (2022). Chitosan and polyhexamethylene guanidine dual-functionalized cotton gauze as a versatile bandage for the management of chronic wounds. Carbohydrate polymers, 282, 119130. https://doi.org/10.1016/j.carbpol.2022.119130

2. Goh, M., Du, M., Peng, W. R., Saw, P. E., & Chen, Z. (2024). Advancing burn wound treatment: exploring hydrogel as a transdermal drug delivery system. Drug delivery, 31(1), 2300945. https://doi.org/10.1080/10717544.2023.2300945

3. Lagoa T, Queiroga MC, Martins L. An Overview of Wound Dressing Materials. Pharmaceuticals (Basel). 2024 Aug 23;17(9):1110. doi: 10.3390/ph17091110. PMID: 39338274; PMCID: PMC11434694.

4. Zhou, X., Liu, C., Han, Y., Li, C., Liu, S., Li, X., Zhao, G., & Jiang, Y. (2022). An antibacterial chitosan-based hydrogel as a potential degradable bio-scaffold for alveolar ridge preservation. RSC Advances 12(50):32219-32229. DOI: 10.1039/D2RA05151F

5. Zöller, K., To, D., & Bernkop-Schnürch, A. (2025). Biomedical applications of functional hydrogels: Innovative developments, relevant clinical trials and

advanced products. Biomaterials, 312, 122718. https://doi.org/10.1016/j.biomaterials.2024.122718

6. García, M. C., Aldana, A. A., Tártara, L. I., Alovero, F., Strumia, M. C., Manzo, R. H., Martinelli, M., & Jimenez-Kairuz, A. F. (2017). Bioadhesive and biocompatible films as wound dressing materials based on a novel dendronized chitosan loaded with ciprofloxacin. Carbohydrate polymers, 175, 75–86. https://doi.org/10.1016/j.carbpol.2017.07.053

7. Kumar, R., Mishra, I., & Kumar, G. (2021). Synthesis and Evaluation of Mechanical Property of Chitosan/PVP Blend Through Nanoindentation-A Nanoscale Study. Journal of Polymers and the Environment. doi:10.1007/s10924-021-02143-0

8. Hasan A, Waibhaw G, Tiwari S et al (2017) Fabrication and characterization of chitosan, polyvinylpyrrolidone, and cellulose nanowhiskers nanocomposite films for wound healing drug delivery application. J Biomed Mater Res A 105:2391–2404. https://doi.org/10.1002/jbm.a.36097

9. Lim JI, Kang MJ, Lee WK (2014) Lotus-leaf-like structured chitosan-polyvinyl pyrrolidone films as an anti-adhesion barrier. Appl Surf Sci 320:614–619. https://doi.org/10.1016/j.apsusc.2014.09.087

10. Lewandowska, K. (2017) Surface properties of chitosan composites with poly(N-vinylpyrrolidone) and montmorillonite. Polym Sci A 59:215–222. https://doi.org/10.1134/S0965545X17020043

11. Li J, Zivanovic S, Davidson PM, Kit K (2010) Characterization and comparison of chitosan/PVP and chitosan/PEO blend films. Carbohydr Polym 79:786–791. https://doi.org/10.1016/j.carbpol.2009.09.028

12. Aldana AA, González A, Strumia MC, Martinelli M (2012) Preparation and characterization of chitosan/genipin / poly (N-vinyl-2-pyrrolidone) films for controlled release drugs. Mater Chem Phys 134:317–324. https://doi.org/10.1016/j.matchemphys.2012.02.071

13. Chen, J., Wei, D., Gong, W., Zheng, A., & Guan, Y. (2018). Hydrogen-Bond Assembly of Poly(vinyl alcohol) and Polyhexamethylene Guanidine for Nonleaching and Transparent Antimicrobial Films. ACS applied materials & interfaces, 10(43), 37535–37543. https://doi.org/10.1021/acsami.8b14238

14. Dias FGG, Pereira LF, Parreira RLT, et al. Evaluation of the antiseptic and wound healing potential of polyhexamethylene guanidine hydrochloride as well as its toxic effects. Eur J Pharm Sci. 2021;160:105739. doi:10.1016/j.ejps.2021.105739

15. Ivanov, I., Kirillova, D., Erimbetov, K., & Shatalov, D. (2024). Toxicity and Safety Analysis of Polyhexamethylene Guanidine: A Comprehensive Systematic Review. Sciences of Pharmacy 3(3), 153-166. doi: 10.58920/sciphar0303263

16. Bainbridge P, Browning P, Bernatchez SF, Blaser C, Hitschmann G. Comparing test methods for moisture-vapor transmission rate (MVTR) for vascular access transparent semipermeable dressings. The Journal of Vascular Access. 2023;24(5):1000-1007. doi:10.1177/11297298211050485

17. Doronina, N., Ivanova, E., Trotsenko, Y., Pshenichnikova, A., Kalinina, E., & Shvets, V. (2005). Methylophilus quaylei sp. nov., a new aerobic obligately methylotrophic bacterium. Systematic and applied microbiology, 28(4), 303–309. https://doi.org/10.1016/j.syapm.2005.02.002

18. Mohamed A.M., Amzaeva D.N., Pshenichnikova A.B., & Shvets V.I. (2018). Influence of polymyxin B on the formation of biofilms by bacterium Methylophilus quaylei on polypropylene and teflon. Fine Chemical Technologies. 13(2):31-39. (In Russ.) https://doi.org/10.32362/2410-6593-2018-13-2-31-39

19. Nation RL, Li J, Cars O, Couet W, Dudley MN, Kaye KS, Mouton JW, Paterson DL, Tam VH, Theuretzbacher U, Tsuji BT, Turnidge JD. Framework for optimisation of the clinical use of colistin and polymyxin B: the Prato polymyxin consensus. Lancet Infect Dis. 2015 Feb;15(2):225-234. doi: 10.1016/S1473-3099(14)70850-3

20. Terekhova, E. A., Stepicheva, N. A., Pshenichnikova, A. B., & Shvets, V. I. (2010). Stearic acid methyl ether: a new extracellular metabolite of the obligate methylotrophic bacterium Methylophilus quaylei. Prikladnaia biokhimiia i mikrobiologiia, 46(2), 180–186. In Russ.

21. Dong, Y., Ruan, Y., Wang, H., Zhao, Y. and Bi, D. (2004), Studies on glass transition temperature of chitosan with four techniques. J. Appl. Polym. Sci., 93: 1553-1558. https://doi.org/10.1002/app.20630

22. Kim S.J., Shin S.R.,. Kim S.I. (2002), Thermal Characterizations of Chitosan and Polyacrylonitrile Semi-Interpenetrating Polymer Networks. High Performance Polymers, 14(3):309-316.

23. Ratto J.A., Hatakeyama T., Blumstein R.B. (1995), Differential scanning calorimetry investigation of phase transitions in water/ chitosan systems. Polymer, 36(15):2915-2919

24. Ogura, K., Kanamoto, T., Itoh, M., Miyashiro, H., & Tanaka, K. (1980). Dynamic mechanical behavior of chitin and chitosan. Polymer Bulletin, 2(5), 301–304. Doi:10.1007/bf00266704

25. Ahn, J.-S., Choi, H.-K., & Cho, C.-S. (2001). A novel mucoadhesive polymer prepared by template

polymerization of acrylic acid in the presence of chitosan. Biomaterials, 22(9), 923–928. Doi:10.1016/s0142-9612(00)00256-8

26. Pizzoli, M., Ceccorulli, G., & Scandola, M. (1991). Molecular motions of chitosan in the solid state. Carbohydrate Research, 222, 205–213. Doi:10.1016/0008-6215(91)89018-b

27. Sakurai, K. (2000). Glass transition temperature of chitosan and miscibility of chitosan/poly(N-vinyl pyrrolidone) blends. Polymer, 41(19), 7051–7056. Doi:10.1016/s0032-3861(00)00067-7

28. Goryunova, P. E., Sologubov, S. S., Markin, A. V., Smirnova, N. N., Zaitsev, S. D., Silina, N. E., & Smirnova, L. A. (2018). Thermodynamic properties of block copolymers of chitosan with poly(D,L-lactide). Thermochimica Acta, 659, 19–26. Doi:10.1016/j.tca.2017.10.024

29. Goryunova, P. E., Sologubov, S. S., Markin, A. V., Smirnova, N. N., Mochalova, A. E., Zaitsev, S. D., & Smirnova, L. A. (2018). Calorimetric study of chitosan-graft-poly(2-ethylhexyl acrylate) copolymer. Thermochimica Acta, 670, 136–141. Doi:10.1016/j.tca.2018.10.023

30. Ur'yash, V.F., Korurina, N.Yu., Larina, V.N., Varlamov, V.P., Grishatova, N.V., Gruzdeva, A.E. (2007). Effect acidolysis on the heat capacity and physical transformations of chitin and chitosan. Vestnik NNGU. №3. In Russ.

31. Lebedeva, N. S., Guseynov, S. S., Yurina, E. S., Vyugin, A. I. (2019). Chitosan: Thermochemical Study. Russian Journal of General Chemistry, 89, 2432–2437. https://doi.org/10.1134/S107036321912017X

32. Khouri, J., Penlidis, A., & Moresoli, C. (2019). Viscoelastic Properties of Crosslinked Chitosan Films. Processes, 7(3), 157. doi:10.3390/pr7030157

33. Rahman L, Goswami J, Choudhury D. Assessment of physical and thermal behaviour of chitosan-based biocomposites reinforced with leaf and stem extract of Tectona grandis. Polymers and Polymer Composites. 2022;30. doi:10.1177/09673911221076305

34. Cristea M, Ionita D, Iftime MM. Dynamic Mechanical Analysis Investigations of PLA-Based Renewable Materials: How Are They Useful? Materials (Basel). 2020 Nov 23;13(22):5302. doi: 10.3390/ma13225302

35. Cona, C.; Bailey, K.; Barker, E. Characterization Methods to Determine Interpenetrating Polymer Network (IPN) in Hydrogels. Polymers 2024, 16, 2050. https://doi.org/10.3390/polym16142050

36. Ebnesajjad S. (2006), Surface Treatment of Materials for Adhesion Bonding. Elsevier Inc.

37. Ryabova V.O., Ayurova O.Zh., Ochirov O.S., Grigor'eva M.N., Stelmakh S.A. Thermomechanical and mechanical properties of biocidal materials based on polyhexamethylene guanidine hydrochloride and polyvinyl alcohol. Proceedings of Universities. Applied Chemistry and Biotechnology. 2024;14(1):27–34. (In Russ.) https://doi.org/10.21285/achb.896.

38. Shatalov, D. O. (2015). Development and standardization of quality control methods for branched oligohexamethyleneguanidine hydrochloride (Doctoral dissertation). Moscow State University of Fine Chemical Technologies named after M.V. Lomonosov, Moscow.

39. Ozerin A. N., Perov N. S., Zelenetsky A. N., Akopova T. A., Ozerina L. A., Kechekyan A. S., Surin N. M., Vladimirov L. V., Yulovskaya V. D. Hybrid nanocomposites based on a graft copolymer of chitosan with polyvinyl alcohol and titanium oxide. Russian Nanotechnologies. T. 4. No. 5–6. 2009. In Russ.

40. Haaf, F., Sanner, A. & Straub, F. (1985). Polymers of N-Vinylpyrrolidone: Synthesis, Characterization and Uses. Polym J 17, 143–152. https://doi.org/10.1295/polymj.17.143

41. Kaçoğlu H.S., Ceylan Ö., Çelebi M. Determination of Swelling Kinetics and Diffusion Mechanisms of Chemically Crosslinked Porous Chitosan Hydrogels. Open Journal of Nano. (2024) 9–2. DOI: 10.56171/ojn.1488770

42. Akakuru OU, Isiuku BO (2017) Chitosan Hydrogels and theirGlutaraldehyde-Crosslinked Counterparts as Potential Drug Release and TissueEngineering Systems - Synthesis, Characterization, Swelling Kinetics andMechanism. J Phys Chem Biophys 7: 256. doi: 10.4172/2161-0398.1000256

43. Norahan MH, Pedroza-González SC, Sánchez-Salazar MG, Álvarez MM, Trujillo de Santiago G. Structural and biological engineering of 3D hydrogels for wound healing. Bioact Mater. 2022 Dec 23;24:197-235. doi: 10.1016/j.bioactmat.2022.11.019

44. Wu P, Fisher AC, Foo PP, Queen D, Gaylor JD. In vitro assessment of water vapour transmission of synthetic wound dressings. Biomaterials. 1995 Feb;16(3):171-5. doi: 10.1016/0142-9612(95)92114-l

45. Federal Agency on Technical Regulating and Metrology. Medical Devices. Adhesive Wound Dressings. General Specifications. GOST R 53498-2019, Moscow: Standartinform, 2019.

How to cite: Ivanov, I., Shatalov, D.. Development of Chitosan-Based Antimicrobial Hydrogel Incorporating Polyvinylpyrrolidone and PHMG. Sciences of Pharmacy. 2024; 3(4):220-229